

Synthesis and Biological Evaluation of the Thionated Antibacterial Agent Nalidixic Acid and Its Organoruthenium(II) Complex

Rosana Hudej,^{†,‡} Jakob Kljun,[†] Wolfgang Kandioller,[§] Urška Repnik,^{||} Boris Turk,^{†,||,⊥} Christian G. Hartinger,^{§,#} Bernhard K. Keppler,[§] Damijan Miklavčič,[‡] and Iztok Turel^{*,†,§}

[†]Faculty of Chemistry and Chemical Technology, University of Ljubljana, Aškerčeva c. 5, SI-1000 Ljubljana, Slovenia

[‡]Faculty of Electrical Engineering, University of Ljubljana, Tržaška c. 25, SI-1000 Ljubljana, Slovenia

[§]Institute of Inorganic Chemistry, University of Vienna, Währinger Straße 42, A-1090 Vienna, Austria

^{||}Jozef Stefan Institute, Jamova c. 39, SI-1000 Ljubljana, Slovenia

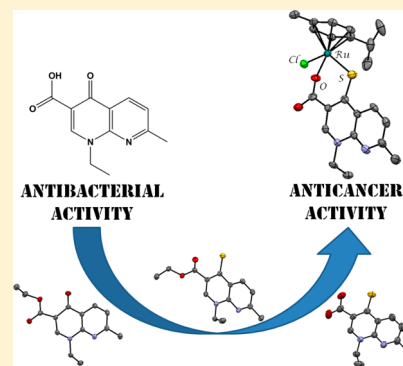
[⊥]CIPKEBIP Centre of Excellence, Jamova c. 39, SI-1000 Ljubljana, Slovenia

[#]School of Chemical Sciences, The University of Auckland, Private Bag 92019, Auckland 1142, New Zealand

[§]EN→Fist Centre of Excellence, Dunajska c. 156, SI-1000 Ljubljana, Slovenia

Supporting Information

ABSTRACT: The thionated derivative of the antibacterial agent nalidixic acid and its organoruthenium complex were prepared, and their crystal structures were determined. The aqueous stability of the complex was studied and, unlike the case for the nalidixicato complex, increased stability of the ruthenium complex in aqueous solution was observed with only a minor degree of thionalidixicato ligand dissociated within 1 week. While the derivatization caused the antibacterial activity of the ligand against *E. coli* to decrease, the cytotoxicity of the complex against three cancer cell lines was significantly increased and the inhibitory potency against two enzymes of the cathepsin family was increased by 10-fold.



1. INTRODUCTION

Transition-metal complexes have played an important role in the treatment of cancer since the discovery of cisplatin in the 1960s.¹ Among the non-platinum compounds, ruthenium complexes have been studied most extensively and two of them, namely NAMI-A and KP1019/KP1339, have successfully entered clinical trials.² Recent developments in the field of ruthenium medicinal chemistry show that organometallic “half-sandwich” ruthenium complexes have promising anticancer activity *in vitro* and *in vivo* (Figure 1).³ Furthermore, the combination of ruthenium chemotherapeutics and electroporation⁴ was shown to be a promising concept, as the antitumor activity of KP1339 (an analogue of KP1019 containing sodium instead of indazolium as the counterion) was enhanced *in vitro* and *in vivo*.⁵ On the other hand, NAMI-A, which is not cytotoxic but is active against metastases in *in vivo* setups, exhibits moderate cytotoxic properties in combination with electroporation.⁶

Many metal complexes have been evaluated as anticancer agents, and also Ru compounds bearing O,O-chelating ligands, which range from simple diketonates or carboxylates to bioactive small molecules, were tested as potential anticancer drugs. It was found that derivatization of the ligand to form

S,O-chelates resulted in metal complexes with increased stability and antiproliferative properties.⁷

Quinolones are a family of synthetic antibacterial agents that possess a β -ketocarboxylate moiety and can thus coordinate to metal cations. Many coordination compounds of metal cations with quinolone ligands display interesting biological properties,⁸ and they are a hot topic in current research.⁹ Notably, the anticancer activity of quinolone derivatives has also been reported.¹⁰

In recent years, it has become evident that interactions with various proteins are of greater importance in the mechanism of action of non-platinum anticancer drugs than binding to DNA.¹² A series of pta-based organoruthenium complexes was therefore evaluated as inhibitors of thioredoxin reductase and cathepsin B, two enzymes that are believed to be important targets in cancer chemotherapy and considered to be highly sensitive to metallodrugs. Cysteine cathepsins are a group of primarily lysosomal proteases, which in humans comprises 11 different enzymes.¹³ The cathepsins were found to have a major

Special Issue: Organometallics in Biology and Medicine

Received: May 17, 2012

Published: July 13, 2012

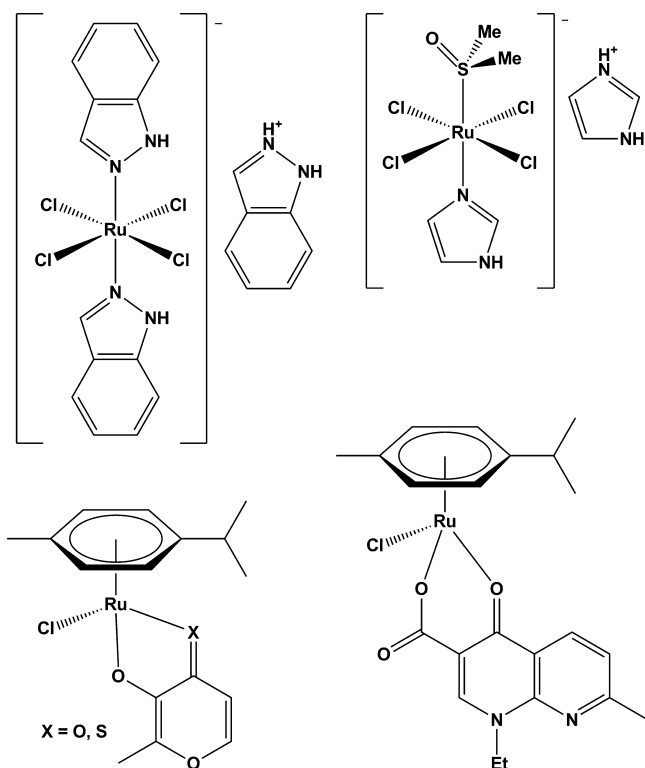
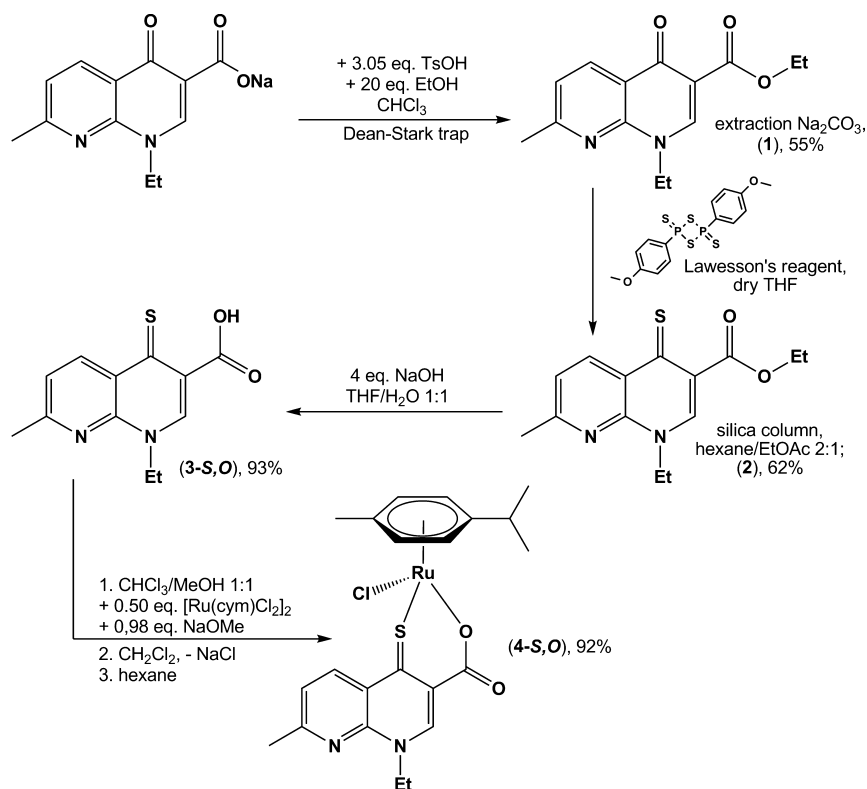


Figure 1. Biologically active ruthenium complexes: (top left) KP1019; (top right) NAMI-A; (bottom left) organoruthenium complex with (thio)maltol;⁷ (bottom right) organoruthenium complex with quinolone nalidixic acid (4-O,O).¹¹

role in a number of diseases, including, cancer, rheumatoid arthritis, atherosclerosis, and osteoporosis.¹⁴ On the basis of animal model studies, genetic ablation of several cathepsins, in particular cathepsins B, S, and L, significantly reduced cancer progression in, for example, the pancreatic islet model and the mammary gland model.¹⁵ Moreover, pharmacological inhibition of cathepsins by broad-spectrum cathepsin inhibitors (i.e., JPM-OEt) also resulted in delayed tumor growth in the same mouse models^{15a,16} or in significant sensitization to other therapies,¹⁷ suggesting that cathepsins are valid targets for anticancer therapy. In addition, intracellular cathepsins are also involved in apoptosis triggering and in autophagy that is promoting tumorigenesis, thereby exhibiting a dual mode of action, which may be of further importance for cancer treatment.¹⁸ Therefore, an active search for molecules that would inhibit cathepsins *in vivo* may be one of the future priorities in anticancer therapy.^{13b,14b} Organoruthenium–pta compounds were found to inhibit cathepsin B with IC_{50} values in the low- μ M range, suggesting that such organometallics may represent a novel class of cathepsin inhibitors that could be used in cancer therapy.¹⁹ In addition to the organoruthenium compounds, organotellurium(IV) compounds²⁰ and cyclo-metallated Pd(II), oxorhenium(V), and gold complexes²¹ were found to be potent inhibitors of various cysteine cathepsins, including cathepsins B, S, V, and K.

Herein, we report the preparation of the thionated derivative of the synthetic antibacterial agent nalidixic acid and its organoruthenium complex. The compounds were characterized using different physicochemical methods, and their crystal structures were determined by single-crystal X-ray diffraction analysis. The antimicrobial activity of the novel nalidixic acid derivative and its organoruthenium complex was evaluated in comparison to the parent compound nalidixic acid and the

Scheme 1. Synthetic Route to Compounds 3-S,O and 4-S,O



related organoruthenium complex (**4-O,O**; see Figure 1). Their cytotoxicity against human cancer cell lines was compared, and the effect of electroporation on cytotoxicity in a murine melanoma cell line was studied.

2. RESULTS AND DISCUSSION

2.1. Syntheses and Characterization. Thionalidixic acid was prepared using sodium nalidixate hydrate as the starting material, which was first converted into the colorless nalidixic acid ethyl ester (**1**) under water-free conditions. Use of a Dean–Stark trap improved the conversion rate from 20–30% to 60–65%. Compound **1** was reacted with Lawesson's reagent in dry THF to give the red thionalidixic acid ethyl ester (**2**). ^1H NMR spectra of crude reaction mixtures showed a conversion rate of 75–80%, which could not be improved either by increasing the reaction time up to 24 h or by using an excess of the thionating reagent. The ester was hydrolyzed under alkaline conditions, and the free thionalidixic acid (**3-S,O**) was precipitated as a yellow powder by dropwise addition of concentrated HCl (Scheme 1). The organoruthenium complex **4-S,O** was obtained by deprotonation of **3-S,O** with sodium methoxide followed by reaction with the ruthenium precursor bis[dichlorido(η^6 -*p*-cymene)ruthenium(II)] (**P1**). After filtration of the byproduct NaCl and other insoluble impurities over Celite, the complex was precipitated from a concentrated dichloromethane solution upon addition of *n*-hexane (Scheme 1) which yielded a red-violet powder.

Crystals suitable for X-ray diffraction analysis were obtained by slow evaporation of ethyl acetate (**1** and **2**), chloroform (**3-S,O**), and dichloromethane/*n*-hexane solutions (**4-S,O**).

Compound **1** exhibits π – π interactions with a distance between planes defined by the atoms of the planar naphthyridine core of 3.426(3) Å and considerable overlap of the stacked molecules. The close packing and the absence of bulkier substituents results in a very narrow unit cell with $a = 4.6074(3)$ Å and a relatively small tilting of the carboxylic group with an angle of 14.24(2)° between planes defined by the aromatic core and the carboxylic carbon and two oxygen atoms. On the other hand, compound **2** presents only weak π – π stacking with the aromatic backbones of the thionalidixic acid ethyl ester molecules, forming a staircase motif, which in turn allows the tilting of the carboxyl group at an angle of 54.90(2)°. The structure of compound **3-S,O** (see Figure 2) features an intramolecular hydrogen bond between the carboxylic acid hydrogen atom and the sulfur atom, which in turn causes the near-coplanarity of the carboxylic group with the aromatic quinolone backbone ($\varphi = 1.18(1)^\circ$). Compound **4-S,O** presents a “piano stool” geometry with a π -bonded cymene, a chlorido ligand, and the thionalidixicato ligand coordinated to the Ru center via the thiocarbonyl sulfur and one carboxylic oxygen (Figure 2).

In comparison with the previously published structures of organometallic ruthenium quinolone complexes, the Ru–cymene centroid distance is longer (1.668(2) Å vs 1.633(3)–1.64(2) Å).¹¹ However, ^1H NMR spectra indicate that in chloroform solution the Ru–cymene bonding is stronger. In comparison to the organoruthenium complex of the non-thionated ligand, a lower chemical shift of one of the doublets corresponding to aromatic cymene protons ($\Delta\delta = -0.16$ ppm) was observed, whereas the shifts assigned to the other group of aromatic cymene hydrogens remain unchanged. The bite angle of the quinolonato ligand is increased as compared to those in structurally related complexes (90.2° vs 85.3–87.3°), which is

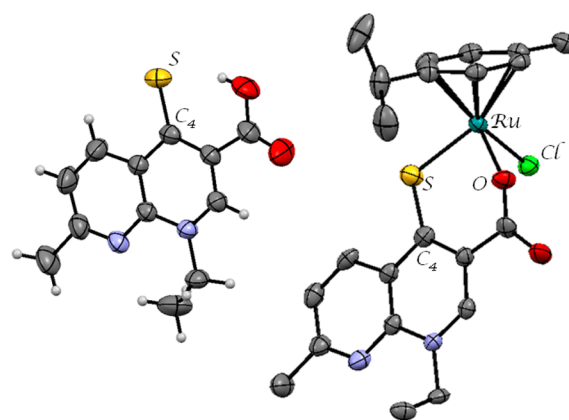


Figure 2. Crystal structures of **3-S,O** (left) and **4-S,O** (right). The ellipsoids are drawn at the 50% probability level, and the hydrogen atoms of **4-S,O** are omitted for clarity. Selected bond lengths (Å): **4-S,O**, Ru–Cl = 2.421(1), Ru–O = 2.069(4), Ru–S = 2.326(2), S–C₄ = 1.680(5); **3-S,O**, S–C₄ = 1.699(2).

explained by the bulkier frame of the ligand. The structure is further stabilized by π – π interactions between partially stacked quinolonato ligands. Additional crystallographic data are provided in the Supporting Information.

The behavior of **4-S,O** in aqueous solution was investigated by means of ^1H NMR spectroscopy. Similar to the case for the previously investigated ruthenium complex bearing nalidixic acid as a ligand, i.e., chlorido(η^6 -*p*-cymene)(nalidixicato- κ^2 -O,O)ruthenium(II) (**4-O,O**),^{11b} the chlorido ligand is quickly released and the aquated species is formed. The aqua species is, in contrast to **4-O,O**, stable in aqueous solution and only a minor release (<3%) of the thioquinolone ligand was observed after 1 week (~50% in the case of **4-O,O**; cf. ref 11b).

2.2. Antimicrobial Activity. The antimicrobial activity of both quinolones (**3-O,O** and **3-S,O**) and their ruthenium complexes (**4-O,O** and **4-S,O**) against the bacterial strain *E. coli* K12 was evaluated using the agar diffusion test. While the nalidixic acid and its ruthenium complex showed moderate activity inhibiting bacterial growth at 40 μM , the thionated derivative and its complex were inactive in the tested concentration range (up to 1 mM). The derivatization of nalidixic acid to thionalidixic acid lowers the antimicrobial activity, which is in agreement with one of the two proposed mechanisms of action for quinolones; this suggests the formation of a magnesium(II) tetraaquaquinolonato complex which binds to the phosphate backbone of bacterial DNA through hydrogen bonds and prevents the replication of bacteria by inhibiting DNA gyrase.²² The lower affinity of the sulfur atom toward magnesium(II) cations in comparison to that toward the oxygen atom may explain the ineffectiveness of the novel derivative. Interestingly, complexation of the quinolone to a ruthenium center does not affect the antimicrobial activity as was the case for other multivalent metal cations, which are commonly found in over-the-counter drugs and/or food supplements such as magnesium, aluminum, calcium, iron, and zinc.^{22b}

2.3. Cytotoxicity. In vitro cytotoxicity assays were performed on human non small cell lung carcinoma (A549), colon adenocarcinoma (SW480), and human ovarian carcinoma (CH1) cells. From the five tested compounds only **4-S,O** showed moderate activity against these human cell lines, while both ligands (**3-O,O** and **4-S,O**), the ruthenium precursor **P1**,

and 4-*O,O* were inactive over the concentration range used ($IC_{50} > 640 \mu\text{M}$) (Table 1).

Table 1. IC_{50} Values (μM) of P1, 3-*S,O* and 4-*S,O* for Different Human Tumor Cell Lines

compd	IC_{50} (μM)		
	A549	CH1	SW480
P1	>640	>640	>640
3- <i>S,O</i>	>640	>640	>640
4- <i>S,O</i>	540 \pm 112	364 \pm 17	302 \pm 24

In order to improve the antiproliferative activity of the complexes, electroporation was applied. Electroporation is a process in which exposing cells to specific electrical pulses results in temporary formation of hydrophilic pores in the cell membrane. Temporally increased cell permeability thus enables extracellular molecules with otherwise hampered transmembrane transport to enter cells. It has been demonstrated that combining electroporation with chemotherapy potentiates the cytotoxicity of drugs when the drug's efficacy is limited by its uptake into the cell. This procedure is clinically approved and is highly effective in the treatment of solid tumors.⁴ Furthermore, promising results were also found when applied in combination with the treatment of cells with ruthenium complexes.^{5,6} However, electroporation did not influence the cytotoxicity of test compounds used in this work. All five compounds were inactive on murine melanoma B16F1 cells with and without electroporation, whereas electroporation improved the cytotoxicity of the ruthenium compounds NAMI-A and KP1339.^{5,6} It needs to be stressed, however, that in vivo antitumor activity of ruthenium compounds cannot always be predicted from in vitro experiments. For example, NAMI-A is not cytotoxic but possesses antimetastatic activity in vivo.^{2e} Subsequent experiments in vivo are thus required to fully evaluate the antitumor activity of the compound class alone and in combination with electroporation.

2.4. Cathepsin Inhibition. The mode of action of ruthenium-based metallodrugs is widely unknown. Due to the presence of a free cysteine in the active site and the ability of various metals to inhibit their activity, cysteine cathepsins have been proposed as potential targets of Ru compounds.^{19,23} Therefore, the inhibitory activity of 4-*O,O* and 4-*S,O* against cathepsin B (CatB) and cathepsin S (CatS), two proteases involved in cancer progression, was evaluated. Recombinant cathepsins B and S were incubated with 4-*O,O* and 4-*S,O* for 14 h, similar to the procedure in previous studies.¹⁹ The ruthenium thionalidixicato complex 4-*S,O* inhibited cathepsins B and S with IC_{50} values of 137 and 66 μM , whereas its nonthionated counterpart 4-*O,O* exhibited essentially no inhibition of the two enzymes. Obviously the replacement of the pyridone O4 by sulfur improved the inhibition of both cathepsins by at least 1 order of magnitude (Table 2).

Due to the very slow inhibition of cathepsin B,¹⁹ the time dependence of cathepsin B and S inhibition was monitored for 24 h (Figure 3). The maximum inhibition of cathepsin B was seen after 24 h, whereas inhibition of cathepsin S was already completed after 14 h, yielding a K_i value of 19.5 μM (Table 3) after a correction for substrate competition (21 μM).²⁴ The inhibition of cathepsin S was thus significantly stronger than that of cathepsin B and was almost comparable to the inhibition of cathepsin B by other organoruthenium compounds.¹⁹ However, a direct comparison of the results is not possible,

Table 2. IC_{50} Values (μM)^a for Inhibition of Recombinant Human CatB and CatS by 4-*O,O* and 4-*S,O*

compd	IC_{50} (μM)	
	CatB	CatS
4- <i>O,O</i>	≥ 800	≥ 800
4- <i>S,O</i>	137 \pm 10	66 \pm 15

^a IC_{50} values are given together with the standard errors.

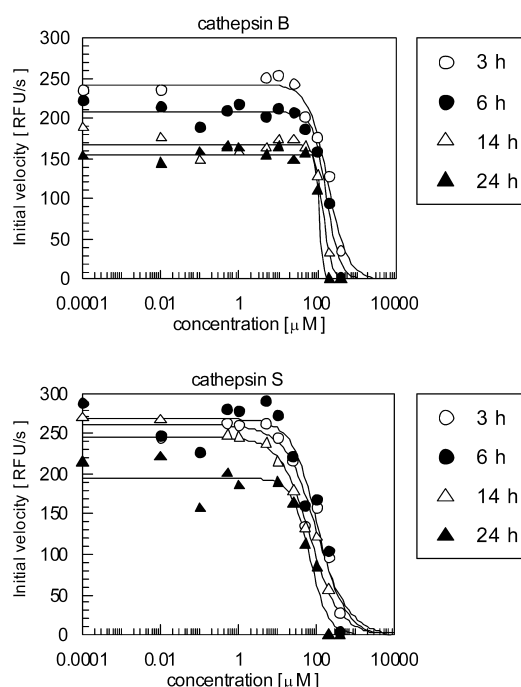


Figure 3. Time dependence of CatB and CatS inhibition by 4-*S,O*. CatB and CatS were incubated with increasing concentrations of 4-*S,O* (10 nM to 400 μM) for 3, 6, 14, and 24 h before measuring the initial velocities of the substrate hydrolysis. For more experimental details see the Experimental Section. The solid lines crossing the experimental data points were calculated with the standard three-parameter equation for IC_{50} calculations using GraFit software (Erithacus Software, U.K.).

Table 3. Time Dependence of Recombinant Human CatB and CatS Inhibition by 4-*S,O* at pH 6.0^a

incubation time (h)	IC_{50} (μM)		K_i (μM) CatS
	CatB	CatS	
3	204 \pm 16	98 \pm 21	
6	167 \pm 14	107 \pm 23	
14	137 \pm 10	66 \pm 15	19.5 \pm 4.4
24	110 \pm 11	66 \pm 12	19.5 \pm 3.6

^aThe experimental conditions are described in the Experimental Section. The best estimates for the IC_{50} values are given together with the standard errors and were calculated as described. K_i values for the inhibition of CatS by 4-*S,O* were also calculated following the correction for substrate competition using a K_m value of 21 μM .²⁴

as only crude cathepsin B extract of bovine origin that may contain other components which could have influenced the inhibition was used in that study.¹⁹ This is, however, substantially lower in comparison to the case for other organometallic compounds, such as gold, tellurium, and

palladium compounds, which exhibit IC_{50} values for cathepsin B in the low μM to nM range.^{20,21}

In addition to the IC_{50}/K_i values, it is important to know how rapidly the inhibitors block the protease activity. A k_2/K_1 value of $\sim 1.00 \pm 0.26 \text{ M}^{-1} \text{ s}^{-1}$ was determined for cathepsin S inhibition by 4-*S,O*, which is almost 10-fold higher than that for cathepsin B ($0.130 \pm 0.068 \text{ M}^{-1} \text{ s}^{-1}$). Although this is substantially slower than inhibition by other well-known cathepsin inhibitors, such as epoxides or some other organometallic compounds,^{20,21} it may still contribute to the antiproliferative effect, especially at relatively high inhibitor concentration. Cysteine cathepsins have a half-life between 14 and 21 h in lysosomes, whereas they are destabilized within 10–90 min at neutral pH, as found in the extracellular space.²⁵ The only exception is CatS, which is quite stable under these conditions.²⁶ It is therefore important to develop inhibitors that act rapidly. Note that inhibition of cysteine cathepsins alone does not trigger cancer cell death. However, blocking the cathepsins *in vivo* by, for example, epoxides significantly slows down tumor growth and invasiveness by blocking the signaling pathways triggered by the cathepsins.¹⁶ Therefore, these results suggest that the potentially beneficial anticancer effect might be a combination of cytotoxicity of the compounds and inhibition of cysteine cathepsins.

3. CONCLUSION

As a part of an ongoing study on ruthenium quinolone complexes and their physicochemical and biological properties, we have successfully devised a synthetic pathway for the preparation of thionated quinolones, where the pyridone oxygen atom is substituted by a sulfur atom. The thionated derivative of nalidixic acid (3-*S,O*) and its organoruthenium complex chlorido(η^6 -*p*-cymene)(thionalidixicato- κ^2 S,O)-ruthenium(II) (4-*S,O*) were thus prepared. As was previously found in the case of complexes bearing hydroxypyrrone ligands,^{3,7} the change of the ruthenium coordination sphere from $\text{Ru}(\eta^6\text{-C}_6\text{ClO}_2)$ to $\text{Ru}(\eta^6\text{-C}_6\text{ClOS})$ led to a significantly more stable complex in aqueous solution with improved cytotoxicity. The novel compound also exhibited a substantial increase by at least 1 order of magnitude in the potency of inhibition of two enzymes, cathepsins B and S, which are involved in various pathological processes, including cancer progression.

4. EXPERIMENTAL SECTION

4.1. Materials and Methods. The starting materials and solvents that were used in the syntheses were purchased from Sigma-Aldrich, Acros Organics, or TCI and were used as received. NMR spectra were recorded at 25 °C using a Bruker Avance III 500 MHz FT-NMR spectrometer. ¹H NMR spectra were measured in DMSO-*d*₆ or CDCl₃ at 500.10 MHz and ¹³C{¹H} NMR spectra at 125.75 MHz. Infrared spectra were recorded with a Perkin-Elmer Spectrum 100 FTIR spectrometer, equipped with a Specac Golden Gate Diamond ATR as a solid sample support. Elemental analyses (C, H, N) were performed with a Perkin-Elmer 2400 Series II CHNS/O analyzer. HRMS were measured on an Agilent 6224 Accurate Mass TOF LC mass spectrometer. X-ray diffraction data for **1** was collected on an Oxford Diffraction SuperNova diffractometer with Mo microfocus X-ray source ($K\alpha$ radiation, $\lambda = 0.71073 \text{ \AA}$) with mirror optics and an Atlas detector. X-ray diffraction data for compounds **2**, 3-*S,O*, and 4-*S,O* were collected on a Nonius Kappa CCD diffractometer equipped with a Mo anode ($K\alpha$ radiation, $\lambda = 0.71073 \text{ \AA}$) and a graphite monochromator at 150(2) K (**2**, 4-*S,O*) and 293(2) K (3-*S,O*). The structures were solved by direct methods implemented in SIR92²⁷ and

refined by a full-matrix least-squares procedure based on F^2 using SHELXL-97.²⁸ All non-hydrogen atoms were refined anisotropically. The hydrogen atoms were placed at calculated positions and treated using appropriate riding models. The programs Mercury, ORTEP, and Platon were used for data analysis and figure preparation.²⁹ The crystal structures of compounds **1**, **2**, 3-*S,O*, and 4-*S,O* have been submitted to the CCDC and have been allocated the deposition numbers CCDC 879554–879557 for compounds 3-*S,O*, **2**, 4-*S,O*, and **1**, respectively.

4.2. Bioassays. **4.2.1. Antimicrobial Activities.** The antimicrobial activities of the test compounds were evaluated on the bacterial strain *Escherichia coli* K12 (ER1821, New England Biolabs) using the agar diffusion test. Bacteria were allowed to grow overnight, and their concentration was then determined. The bacterial culture was incorporated into Luria Broth nutrient agar with the final concentration of bacteria being approximately 10^7 CFU/mL (colony forming unit per mL). Inoculated medium (20 mL) was poured into Petri dishes and kept at 4 °C until use. Circles of agar (0.8 cm) were cut out from the cooled medium. The MIC (minimal inhibitory concentration) values of thionalidixic acid, sodium nalidixicate, and 4-*S,O* were determined, using nalidixic acid as a reference substance. MIC represents the lowest concentration of an antibiotic that inhibits the growth of a tested organism. For estimating the MIC, the antibacterial substances were diluted gradually in distilled water. A 100 μL portion of each dilution was poured into the holes cut into the inoculated medium, and the system was kept at 37 °C for 24 h. Finally, the plates were examined for the occurrence of inhibition zones.

4.2.2. Cytotoxicity. The human non small cell lung carcinoma (A549) and colon adenocarcinoma (SW480) cell lines were provided by Brigitte Marian (Institute of Cancer Research, Department of Medicine I, Medical University of Vienna, Austria). The human ovarian carcinoma cell line CH1 was a gift from Lloyd R. Kelland (CRC Centre for Cancer Therapeutics, Institute of Cancer Research, Sutton, U.K.). Cells were grown in 75 cm² culture flasks (Iwaki/Asahi Technoglass, Gyouda, Japan) in complete medium (Minimum Essential Medium supplemented with 10% heat-inactivated fetal bovine serum, 1 mM sodium pyruvate, 4 mM L-glutamine, and 1% nonessential amino acids (100 \times)) as adherent monolayer cultures. All media and supplements were purchased from Sigma-Aldrich (Vienna, Austria). Cultures were maintained at 37 °C under a humidified atmosphere containing 5% CO₂.

Cytotoxicity was determined by a colorimetric assay (MTT assay, MTT = 3-(4,5-dimethyl-2-thiazolyl)-2,5-diphenyl-2H-tetrazolium bromide, Fluka). For this purpose, cells were harvested from culture flasks by trypsinization and seeded in 100 μL per well into 96-well plates (Iwaki/Asahi Technoglass, Gyouda, Japan) in cell densities of 4×10^3 (A549), 1.5×10^3 (CH1), and 2.5×10^3 cells per well (SW480), respectively. These cell numbers ensure exponential growth of untreated controls throughout drug exposure of treated microcultures. Cells were allowed to adhere and resume proliferation in drug-free complete culture medium for 24 h. Drugs were dissolved in complete medium and appropriately diluted, and instantly 100 μL of the drug dilutions was added per well. After exposure for 96 h at 37 °C and 5% CO₂, drug solutions were replaced by 100 μL /well RPMI 1640 culture medium (supplemented with 10% heat-inactivated fetal bovine serum and 4 mM L-glutamine) plus 20 μL /well MTT solution in phosphate-buffered saline (5 mg/mL) and incubated for 4 h. Subsequently, the medium/MTT mixture was removed and the formazan crystals that were formed in vital cells were dissolved in 150 μL of DMSO (dimethyl sulfoxide) per well. Optical densities were measured with a microplate reader (Tecan Spectra Classic) at 550 nm (and a reference wavelength of 690 nm) to yield relative quantities of viable cells as percentages of untreated controls, and 50% inhibitory concentrations (IC_{50}) were calculated from concentration-effect curves by interpolation. Calculations are based on at least three independent experiments, each consisting of three replicates per concentration level.

4.2.3. Electroporation Experiments. The cytotoxicity of the test compounds was determined on the murine melanoma cell line B16F1 (European Collection of Cell Cultures, U.K.) in combination with or without electroporation. Cell suspensions were prepared from

confluent cell cultures by trypsinization. The final concentration of cells in 0.9% NaCl was 2.2×10^7 cells/mL. The test compounds were dissolved in 0.9% NaCl and prepared in concentrations from 0 to 1 mM. The compounds were added to the cell suspensions to reach final concentrations of 0, 0.01, and 0.1 mM. Immediately after incubation (<0.5 min), a drop of cell suspension was placed between two flat parallel stainless-steel electrodes 2 mm apart. A train of electric rectangular unipolar pulses (8 pulses, 800 V/cm, 100 μ s, 1 Hz) was applied with an Cliniporator electroporator (Igea, Carpi, Italy). The same procedure without electric pulses was used for cells exposed to the tested compounds only. In addition, we tested the cytotoxicity of compounds after prolonged incubation time (60 min, without electroporation). Nonelectroporated cells incubated in 0.9% NaCl served as controls (c). Cell viability was measured 72 h after treatment using the MTS-based Cell Titer 96 AQueous One Solution Cell Proliferation Assay (Promega, USA). Absorption at 490 nm wavelength (A_{490}) was measured with a Tecan Infinite M200 spectrophotometer (Tecan, Switzerland). Statistical analysis was performed using One-Way ANOVA test and SigmaPlot v. 11.0 statistical software (SPSS, Chicago, IL).

4.2.4. Cathepsin Inhibition Assays. Initial solutions of 50 mM 4-*O*,*O* and 10 mM 4-*S*,*O* were prepared in DMSO. Final DMSO concentrations never exceeded 4% (v/v), which does normally not affect cathepsin activity. Subsequent dilutions were made in 100 mM phosphate buffer, pH 6.0. Recombinant human cathepsins were prepared as described earlier³⁰ in *E. coli* (CatB)³¹ or *P. pastoris* (CatS)³² expression systems. The assay buffer for enzyme kinetics measurements was 100 mM sodium phosphate, pH 6.0, supplemented with 1 mM EDTA, 0.1% (w/v) polyethylene glycol (PEG), and 1 mM dithiothreitol (DTT). The experimental conditions, i.e. pH 6.0 and the use of PEG, were selected in order to improve the stability of the enzymes and to minimize protein adsorption to the surface. Cathepsins were activated in the assay buffer supplemented with 5 mM DTT for 5 min at room temperature. The cleavage of the fluorogenic substrate Z-Phe-Arg-AMC (Bachem) was used to assess the enzyme activity. Kinetic measurements were performed with a fixed cathepsin concentration of 25 nM and a fixed substrate concentration of 50 μ M. Inhibitor concentrations ranged from 10 nM to 400 μ M: 10 nM/100 nM/500 nM/1 μ M/5 μ M/10 μ M/25 μ M/50 μ M/100 μ M/200 μ M/400 μ M. Prior to the addition of substrate, compounds were incubated with CatB or CatS for the designated time (3–24 h) at room temperature. Cathepsin activity was then measured at room temperature over 3 min at excitation and emission wavelengths of 370 and 460 nm, respectively. All measurements were performed in duplicate, using a Tecan Sapphire plate reader (Tecan Group, Switzerland). Initial velocities of the enzyme activity reactions were calculated and plotted against the inhibitor concentrations. IC_{50} values were calculated using the standard three-parameter equation for determination of IC_{50} values by the GraFit program (Erithacus Software, U.K.). The k_2/K_1 (association rate constant) values for the interaction between both cathepsins and 4-*S*,*O* were then calculated from the IC_{50} curves using the assumption that this is a pseudo-first-order reaction with a large excess of the inhibitor. Due to a significant loss of activity observed for both enzymes, especially at the 24 h time point (30–40%; Figure 3), a correction for spontaneous inactivation of the enzymes was necessary.

4.3. Syntheses and Characterization. **4.3.1. Nalidixic Acid Ethyl Ester (1; $C_{14}H_{16}N_2O_3$).** Sodium nalidixate hydrate (500 mg, 1.84 mmol, 1 equiv) was suspended in 40 mL of chloroform, and *p*-toluenesulfonic acid hydrate (1067 mg, 5.61 mmol, 3.05 equiv) and 1 mL of ethanol were added. The reaction mixture was refluxed overnight. The crude product was treated with approximately 20 mL of saturated sodium carbonate solution in a separation funnel. The organic layer was collected, washed with distilled water (2×10 mL), and dried with sodium sulfate, and the solvent was removed under vacuum (291 mg; 55%). Single crystals suitable for X-ray diffraction analysis were obtained by slow evaporation of an ethyl acetate solution. 1H NMR (DMSO- d_6 , 500.10 MHz, 25 $^\circ C$): δ 8.81 (s, 1H, H2), 8.44 (d, $^3J(H,H) = 8$ Hz, 1H, H5), 7.41 (d, $^3J(H,H) = 8$ Hz, 1H, H6), 4.48 (q, $^3J(H,H) = 8$ Hz, 2H, NCH_2CH_3), 4.23 (q, $^3J(H,H) = 8$

Hz, 2H, OCH_2CH_3), 2.63 (s, 3H, $ArCH_3$), 1.37 (t, $^3J(H,H) = 8$ Hz, 3H, NCH_2CH_3), 1.29 (t, $^3J(H,H) = 8$ Hz, 3H, OCH_2CH_3). ^{13}C NMR (DMSO- d_6 , 126 MHz): δ 173.1, 164.3, 162.4, 149.1, 148.2, 135.9, 121.0, 120.5, 111.2, 59.8, 45.6, 24.6, 14.8, 14.3. IR (cm^{-1} , ATR): 2991, 1682, 1625, 1604, 1544, 1439, 1255, 1209, 1092, 799. HRMS-ESI (m/z): $[M + H]^+$ calcd for $C_{14}H_{17}N_2O_3$ 261.1239, found 261.1235. Anal. Calcd for $C_{14}H_{16}N_2O_3$: C, 64.60; H, 6.20; N, 10.77. Found: C, 64.33; H, 6.57; N, 11.02.

4.3.2. Thionalidixic Acid Ethyl Ester (2; $C_{14}H_{16}N_2O_2S$). Compound 1 (250 mg, 0.91 mmol, 1 equiv) and Lawesson's reagent (213 mg, 0.50 mmol, 1.1 equiv) were suspended in 10 mL of dry THF. The suspension was refluxed under argon for 5 h. After a few minutes the suspension turned into a deep red solution. Compound 2 was isolated from the reaction mixture on a silica column using a *n*-hexane/ethyl acetate (2/1) mixture as eluent ($R_f = 0.65$, 164 mg, 62%). Single crystals suitable for X-ray diffraction analysis were obtained by slow evaporation of an ethyl acetate solution. 1H NMR (DMSO- d_6 , 500.10 MHz, 25 $^\circ C$): δ 8.94 (d, $^3J(H,H) = 8$ Hz, 1H, H5), 8.55 (s, 1H, H2), 7.50 (d, $^3J(H,H) = 8$ Hz, 1H, H6), 4.52 (q, $^3J(H,H) = 8$ Hz, 2H, NCH_2CH_3), 4.27 (q, $^3J(H,H) = 8$ Hz, 2H, OCH_2CH_3), 2.65 (s, 3H, $ArCH_3$), 1.41 (t, $^3J(H,H) = 8$ Hz, 3H, NCH_2CH_3), 1.30 (t, $^3J(H,H) = 8$ Hz, 3H, OCH_2CH_3). ^{13}C NMR (DMSO- d_6 , 126 MHz): δ 190.4, 165.9, 163.6, 144.1, 139.4, 138.7, 128.5, 127.2, 122.8, 60.8, 46.4, 24.8, 14.9, 14.0. IR (cm^{-1} , ATR): 2986, 1723, 1600, 1439, 1368, 1267, 1176, 1123, 1046, 785. HRMS-ESI (m/z): $[M + H]^+$ calcd for $C_{14}H_{17}N_2O_2S$ 277.1011, found 277.1009. Anal. Calcd for $C_{14}H_{16}N_2O_2S$: C, 60.85; H, 5.84; N, 10.14. Found: C, 61.11; H, 5.99; N, 10.02.

4.3.3. Thionalidixic Acid (3-*S*,*O*; $C_{12}H_{12}N_2O_2S$). Compound 2 (200 mg, 0.72 mmol, 1 equiv) and NaOH (115 mg, 2.88 mmol, 4 equiv) were dissolved in 30 mL of a THF/water (1/1) mixture and stirred vigorously for 2 h at room temperature. Concentrated HCl was added dropwise until a yellow precipitate formed (167 mg, 93%). Single crystals of 3-*S*,*O* suitable for X-ray diffraction analysis were obtained by slow evaporation of a chloroform solution. 1H NMR (DMSO- d_6 , 500.10 MHz, 25 $^\circ C$): δ 15.07 (s, 1H, OH), 9.35 (s, 1H, H2), 9.08 (d, $^3J(H,H) = 8$ Hz, 1H, H5), 7.71 (d, $^3J(H,H) = 8$ Hz, 1H, H6), 4.74 (q, $^3J(H,H) = 8$ Hz, 2H, NCH_2CH_3), 2.73 (s, 3H, $ArCH_3$), 1.46 (t, $^3J(H,H) = 8$ Hz, 3H, NCH_2CH_3). ^{13}C NMR (DMSO- d_6 , 126 MHz): δ 187.6, 166.0, 165.2, 146.8, 143.8, 138.7, 126.4, 124.2, 121.7, 48.0, 24.9, 15.0. IR (cm^{-1} , ATR): 3061, 2976, 2391, 1701, 1597, 1422, 1364, 1343, 1126, 786. HRMS-ESI (m/z): $[M + H]^+$ calcd. for $C_{12}H_{13}N_2O_2S$ 249.0698, found: 249.0695. Anal. Calcd for $C_{12}H_{12}N_2O_2S$: C, 58.05; H, 4.87; N, 11.27. Found: C, 57.87; H, 5.01; N, 11.39.

4.3.4. Chlorido(η^6 -*p*-cymene)(thionalidixicato- κ^2 -*S*,*O*)ruthenium(III) (4-*S*,*O*; $C_{22}H_{25}ClN_2O_2RuS$). $[Ru(\eta^6$ -*p*-cymene)Cl(μ -Cl)]₂ (40.0 mg, 0.065 mmol, 0.5 equiv), 3-*S*,*O* (32.4 mg, 0.130 mmol), and NaOMe (6.9 mg, 0.128 mmol, 0.98 equiv) were dissolved in 25 mL of a MeOH/chloroform (1/1) mixture and refluxed overnight under an argon atmosphere. The solvent was evaporated, and the remaining solid was dissolved in dichloromethane and filtered over Celite to remove NaCl and other insoluble impurities. The solution was concentrated to 3 mL, and the product (4-*S*,*O*; 55.4 mg, 82%) was precipitated by addition of hexane (20 mL). Single crystals of 4-*S*,*O* suitable for X-ray diffraction analysis were obtained by slow evaporation of a dichloromethane/*n*-hexane (1/1) solution. 1H NMR ($CDCl_3$, 500.10 MHz, 25 $^\circ C$): δ 9.18 (d, 1H, $^3J(H,H) = 8$ Hz, H5), 9.14 (s, 1H, H2), 7.45 (d, $^3J(H,H) = 8$ Hz, 1H, H6), 5.48–5.33 (m, 4H, ArH cymene), 4.70–4.65 (m, 2H, NCH_2CH_3), 2.97–2.88 (m, 1H, $ArCH(CH_3)_2$ cymene), 2.74 (s, 3H, $ArCH_3$ nalidixic), 2.16 (s, 3H, $ArCH_3$ cymene), 1.58 (t, 2H, $^3J(H,H) = 8$ Hz, NCH_2CH_3), 1.20 (d, 6H, $^3J(H,H) = 7$ Hz, $ArCH(CH_3)_2$ cymene). ^{13}C NMR (DMSO- d_6 , 126 MHz): δ 179.8, 165.8, 163.6, 146.0, 141.7, 137.4, 124.1, 122.3, 101.7, 99.4, 83.4, 82.8, 80.6, 79.5, 47.6, 29.6, 24.2, 21.7, 21.2, 17.3, 14.3. IR (cm^{-1} , ATR): 2963, 1618, 1599, 1447, 1352, 1337, 1249, 1117, 1027, 793. HRMS-ESI (m/z): $[M - Cl]^+$ calcd for $C_{22}H_{25}N_2O_2RuS$ 483.0680, found 483.0679. Anal. Calcd for $C_{22}H_{25}ClN_2O_2RuS$: C, 51.01; H, 4.87; N, 5.41. Found: C, 51.31; H, 4.42; N, 5.72.

4.4. Aquation Experiments. Complex **4** (1–2 mg/mL) was dissolved in 10% DMSO- d_6 /D $_2$ O, and 1 H NMR spectra were recorded immediately after dissolution, after 24 h, and after 1 week.

■ ASSOCIATED CONTENT

■ Supporting Information

A table and CIF files giving crystallographic data for **1**, **2**, **3-S,O**, and **4-S,O** and figures giving crystal structures of compounds **1** and **2** and a numbering scheme for NMR assignments. This material is available free of charge via the Internet at <http://pubs.acs.org>.

■ AUTHOR INFORMATION

Corresponding Author

*Fax: (+) 386 1 24 19 220. E-mail: iztok.turel@fkk.uni-lj.si.

Notes

The authors declare no competing financial interest.

■ ACKNOWLEDGMENTS

We are grateful for financial support from a bilateral Slovenian–Austrian project, project J1-4131 (I.T.), junior researcher grants for R.H. and J.K., and the program grant PI-0140 (B.T.) of the Slovenian Research Agency (ARRS). We acknowledge the support of the Mahlke-Obermann Foundation, the Hochschuljubiläumsstiftung Vienna and the Austrian Exchange Service (ÖAD). The project was also supported by COST D39 and COST CM1105, in particular by a short-term scientific mission (STSM D39-6067) for J.K. We thank Amalija Golobič and Marta Kasunič for help and advice in crystal structure solution and refinement. We thank Duša Hodžić for help and insights on the laboratory work with bacterial strains and Dr. Michael Jakupec and the cell biology team of the Institute of Inorganic Chemistry at the University of Vienna for conducting the MTT assays.

■ REFERENCES

- (1) (a) Rosenberg, B.; Vancamp, L.; Trosko, J. E.; Mansour, V. H. *Nature* **1969**, *222*, 385–386. (b) Jakupec, M. A.; Galanski, M.; Arion, V. B.; Hartinger, C. G.; Keppler, B. K. *Dalton Trans.* **2008**, 183–194.
- (2) (a) Rademaker-Lakhai, J. M.; van den Bongard, D.; Pluim, D.; Beijnen, J. H.; Schellens, J. H. M. *Clin. Cancer Res.* **2004**, *10*, 3717–372. (b) Hartinger, C. G.; Zorbas-Seifried, S.; Jakupec, M. A.; Kynast, B.; Zorbas, H.; Keppler, B. K. *J. Inorg. Biochem.* **2006**, *100*, 891–904. (c) Sava, G.; Alessio, E.; Bergamo, A.; Mestroni, G. In *Topics in Biological Inorganic Chemistry*; Clarke, M. J., Sadler, P. J., Eds.; Springer-Verlag: Berlin, 1999; pp 143–169. (d) Bratsos, I.; Gianferrara, T.; Alessio, E.; Hartinger, C. G.; Jakupec, M. A.; Keppler, B. K. In *Bioinorganic Medicinal Chemistry*; Alessio, E., Ed.; Wiley-VCH: Weinheim, Germany, 2011; 10.1002/9783527633104.ch5. (e) Dyson, P. J.; Sava, G. *Dalton Trans.* **2006**, 16, 1929–1933.
- (3) Ang, W. H.; Casini, A.; Sava, G.; Dyson, P. J. *J. Organomet. Chem.* **2011**, *696*, 989–998.
- (4) (a) Teissie, J.; Golzio, M.; Rols, M. P. *Biochim. Biophys. Acta* **2005**, *1724*, 270–280. (b) Pavlin, M.; Miklavčič, D. *Bioelectrochemistry* **2008**, *74*, 38–46. (c) Serša, G.; Čemažar, M.; Miklavčič, D. *Cancer Res.* **1995**, *55*, 3450–3455. (d) Testori, A.; Rossi, C. R.; Tosti, G. *Curr. Opin. Oncol.* **2012**, *24*, 155–161. (e) Edhemovic, I.; Gadzjev, E. M.; Breclj, E.; Miklavcic, D.; Kos, B.; Zupanic, A.; Mali, B.; Jarm, T.; Pavliha, D.; Marcan, M.; Gasljevic, G.; Gorjup, V.; Music, M.; Vavpotic, T. P.; Cemazar, M.; Snoj, M.; Sersa, G. *Tech. Cancer Res. Treat.* **2011**, *10*, 475–485.
- (5) Hudej, R.; Turel, I.; Kandušer, M.; Ščančar, J.; Kranjc, S.; Serša, G.; Miklavčič, D.; Jakupec, M. A.; Keppler, B. K.; Čemažar, M. *Anticancer Res.* **2010**, *30*, 2055–2063.

(6) Biček, A.; Turel, I.; Kandušer, M.; Miklavčič, D. *Bioelectrochemistry* **2007**, *71*, 113–117.

(7) (a) Hanif, M.; Henke, H.; Meier, S. M.; Martic, S.; Labib, M.; Kandioller, W.; Jakupec, M. A.; Arion, V. B.; Kraatz, H. B.; Keppler, B. K.; Hartinger, C. G. *Inorg. Chem.* **2010**, *49*, 7953–7963. (b) Mendoza-Ferri, M. G.; Hartinger, C. G.; Mendoza, M. A.; Groessl, M.; Egger, A. E.; Eichinger, R. E.; Mangrum, J. B.; Farrell, N. P.; Maruszak, M.; Bednarski, P. J.; Klein, F.; Jakupec, M. A.; Nazarov, A. A.; Severin, K.; Keppler, B. K. *J. Med. Chem.* **2009**, *52*, 916–925. (c) Peacock, A. F. A.; Melchart, M.; Deeth, R. J.; Habtemariam, A.; Parsons, S.; Sadler, P. J. *Chem. Eur. J.* **2007**, *13*, 2601–2613. (d) Melchart, M.; Habtemariam, A.; Parsons, S.; Sadler, P. J. *J. Inorg. Biochem.* **2007**, *101*, 1903–1912. (e) Kandioller, W.; Hartinger, C. G.; Nazarov, A. A.; Kuznetsov, M. L.; John, R. O.; Bartel, C.; Jakupec, M. A.; Arion, V. B.; Keppler, B. K. *Organometallics* **2009**, *28*, 4249–4251. (f) Kandioller, W.; Hartinger, C. G.; Nazarov, A. A.; Bartel, C.; Skocic, M.; Jakupec, M. A.; Arion, V. B.; Keppler, B. K. *Chem. Eur. J.* **2009**, *15*, 12283–12291.

(8) Turel, I. *Coord. Chem. Rev.* **2002**, *232*, 27–47.

(9) (a) Skyrianou, K. C.; Perdih, F.; Papadopoulos, A. N.; Turel, I.; Kessissoglou, D. P.; Psomas, G. *J. Inorg. Biochem.* **2011**, *105*, 1273–1285. (b) Tarushi, A.; Polatoglou, E.; Kljun, J.; Turel, I.; Psomas, G.; Kessissoglou, D. P. *Dalton Trans.* **2011**, *40*, 9461–9473. (c) Saraiva, R.; Lopes, S.; Ferreira, M.; Novais, F.; Pereira, E.; Feio, M. J.; Gameiro, P. *J. Inorg. Biochem.* **2010**, *104*, 843–850.

(10) (a) Fan, J. Y.; Sun, D.; Yu, H. T.; Kerwin, S. M.; Hurley, L. H. *J. Med. Chem.* **1995**, *38*, 408–424. (b) Zeng, Q. P.; Kwok, Y.; Kerwin, S. M.; Mangold, G.; Hurley, L. H. *J. Med. Chem.* **1998**, *41*, 4273–4278.

(11) (a) Turel, I.; Kljun, J.; Perdih, F.; Morozova, E.; Bakulev, V.; Kasyanenko, N.; Byl, J. A. W.; Osheroff, N. *Inorg. Chem.* **2010**, *49*, 10750–10752. (b) Kljun, J.; Bytzeck, A. K.; Kandioller, W.; Bartel, C.; Jakupec, M. A.; Hartinger, C. G.; Keppler, B. K.; Turel, I. *Organometallics* **2011**, *30*, 2506–2512.

(12) (a) Casini, A.; Hartinger, C. G.; Gabbiani, C.; Mini, E.; Dyson, P. J.; Keppler, B. K.; Messori, L. *J. Inorg. Biochem.* **2008**, *102*, 564–575. (b) Ang, W. H.; De Luca, A.; Chapuis-Bernasconi, C.; Juillerat-Jeanneret, L.; Lo Bello, M.; Dyson, P. J. *ChemMedChem* **2007**, *2*, 1799–1806. (c) Casini, A.; Mastrobuoni, G.; Ang, W. H.; Gabbiani, C.; Pieraccini, G.; Moneti, G.; Dyson, P. J.; Messori, L. *ChemMedChem* **2007**, *2*, 631–635.

(13) (a) Turk, B.; Turk, V. *J. Biol. Chem.* **2009**, *284*, 21783–21787. (b) Repnik, U.; Stoka, V.; Turk, V.; Turk, B. *Biochim. Biophys. Acta* **2012**, *1824*, 22–33.

(14) (a) Mohamed, M. M.; Sloane, B. F. *Nat. Rev. Cancer* **2006**, *6*, 764–775. (b) Vasiljeva, O.; Reinheckel, T.; Peters, C.; Turk, D.; Turk, V.; Turk, B. *Curr. Pharm. Des.* **2007**, *13*, 387–403. (c) Joyce, J. A.; Pollard, J. W. *Nat. Rev. Cancer* **2009**, *9*, 239–252. (d) Reiser, J.; Adair, B.; Reinheckel, T. *J. Clin. Invest.* **2010**, *120*, 3421–3431.

(15) (a) Gocheva, V.; Zeng, W.; Ke, D. X.; Klimstra, D.; Reinheckel, T.; Peters, C.; Hanahan, D.; Joyce, J. A. *Genes Dev.* **2006**, *20*, 543–556. (b) Vasiljeva, O.; Korovin, M.; Gajda, M.; Brodoefel, H.; Bojic, L.; Kruger, A.; Schurigt, U.; Sevenich, L.; Turk, B.; Peters, C.; Reinheckel, T. *Oncogene* **2008**, *27*, 4191–4199.

(16) (a) Joyce, J. A.; Baruch, A.; Chehade, K.; Meyer-Morse, N.; Giraud, E.; Tsai, F. Y.; Greenbaum, D. C.; Hager, J. H.; Bogyo, M.; Hanahan, D. *Cancer Cell* **2004**, *5*, 443–453. (b) Mikhaylov, G.; Mikac, U.; Magaeva, A. A.; Itin, V. I.; Naiden, E. P.; Psakhye, I.; Babes, L.; Reinheckel, T.; Peters, C.; Zeiser, R.; Bogyo, M.; Turk, V.; Psakhye, S. G.; Turk, B.; Vasiljeva, O. *Nat. Nanotech.* **2011**, *6*, 594–602.

(17) Shree, T.; Olson, O. C.; Elie, B. T.; Kester, J. C.; Garfall, A. L.; Simpson, K.; Bell-McGuinn, K. M.; Zabor, E. C.; Brogi, E.; Joyce, J. A. *Genes Dev.* **2011**, *25*, 2465–2479.

(18) Repnik, U.; Turk, B. *Mitochondrion* **2010**, *10*, 662–669.

(19) Casini, A.; Gabbiani, C.; Sorrentino, F.; Rigobello, M. P.; Bindoli, A.; Geldbach, T. J.; Marrone, A.; Re, N.; Hartinger, C. G.; Dyson, P. J.; Messori, L. *J. Med. Chem.* **2008**, *51*, 6773–6781.

(20) (a) Cunha, R. L. O. R.; Urano, M. E.; Chagas, J. R.; Almeida, P. C.; Bincoletto, C.; Tersariol, I. L. S.; Comasseto, J. V. *Bioorg. Med. Chem. Lett.* **2005**, *15*, 755–760. (b) Piovan, L.; Alves, M. F. M.; Juliano, L.; Brömme, D.; Cunha, R. L. O. R.; Andrade, L. H. *Bioorg.*

Med. Chem. **2011**, *19*, 2009–2014. (c) Caracelli, I.; Vega-Tejido, M.; Zuckerman-Schpector, J.; Cezari, M. H. S.; Lopes, J. G. S.; Juliano, L.; Santos, P. S.; Comasseto, J. V.; Cunha, R. L. O. R.; Tiekink, E. R. T. *J. Mol. Struct.* **2012**, *1013*, 11–18.

(21) (a) Mosi, R.; Baird, I. R.; Cox, J.; Anastassov, V.; Cameron, B.; Skerlj, R. T.; Fricker, S. P. *J. Med. Chem.* **2006**, *49*, 5262–5272. (b) Fricker, S. P. *Metallomics* **2010**, *2*, 366–377. (c) Zhu, Y.; Cameron, B. R.; Mosi, R.; Anastassov, V.; Cox, J.; Qin, L.; Santucci, Z.; Metz, M.; Skerlj, R. T.; Fricker, S. P. *J. Inorg. Biochem.* **2011**, *105*, 754–762.

(22) (a) Andriole, V. T., Ed. *The quinolones*, 3rd ed.; Academic Press: San Diego, CA, 2000. (b) Qaqish, R.; Polk, R. E. In *Quinolone Antibacterial Agents*, 3rd ed.; Hooper, D. C., Rubinstein, E., Ed.; ASM Press: Washington, DC, 2003; Chapter 7, pp 133–146.

(23) Mura, P.; Camalli, M.; Casini, A.; Gabbiani, C.; Messori, L. *J. Inorg. Biochem.* **2010**, *104*, 111–117.

(24) Bromme, D.; Bonneau, P. R.; Lachance, P.; Wiederanders, B.; Kirsche, H.; Peters, C.; Thomas, D. Y.; Storer, A. C.; Vernet, T. *J. Biol. Chem.* **1993**, *268*, 4832–4838.

(25) (a) Kominami, E.; Tsukahara, T.; Bando, Y.; Katunuma, N. *Biochem. Biophys. Res. Commun.* **1987**, *144*, 749–756. (b) Nissler, K.; Strubel, W.; Kreuzsch, S.; Rommerskirch, W.; Weber, E.; Wiederanders, B. *Eur. J. Biochem.* **1999**, *263*, 717–725. (c) Turk, B.; Dolenc, I.; Turk, V.; Bieth, J. G. *Biochemistry* **1993**, *32*, 375–380. (d) Turk, B.; Dolenc, I.; Zerovnik, E.; Turk, D.; Gubensek, F.; Turk, V. *Biochemistry* **1994**, *33*, 14800–14806. (e) Dehrmann, F. M.; Elliott, E.; Dennison, C. *Biol. Chem. Hoppe Seyler* **1996**, *377*, 391–394.

(26) Kirschke, H.; Wiederanders, B.; Bromme, D.; Rinne, A. *Biochem. J.* **1989**, *264*, 467–473.

(27) Altomare, A.; Burla, M. C.; Camalli, M.; Cascarano, G. L.; Giacobozzo, C.; Guagliardi, A.; Moliterni, A. G. G.; Polidori, G.; Spagna, R. *J. Appl. Crystallogr.* **1999**, *32*, 115–119.

(28) Sheldrick, G. M. *Acta Crystallogr., Sect. A: Found. Crystallogr.* **2008**, *A64*, 112–122.

(29) (a) Macrae, C. F.; Edgington, P. R.; McCabe, P.; Pidcock, E.; Shields, G. P.; Taylor, R.; Towler, M.; van de Streek, J. *J. Appl. Crystallogr.* **2006**, *39*, 453–457. (b) Faruggia, L. J. *J. Appl. Crystallogr.* **1997**, *30*, 565. (c) Spek, A. L. *J. Appl. Crystallogr.* **2003**, *36*, 7–13.

(30) Bromme, D.; Nallaseth, F. S.; Turk, B. *Methods* **2004**, *32*, 199–206.

(31) Rozman, J.; Stojan, J.; Kuhelj, R.; Turk, V.; Turk, B. *FEBS Lett.* **1999**, *459*, 358–362.

(32) Mihelic, M.; Dobersek, A.; Guncar, G.; Turk, D. *J. Biol. Chem.* **2008**, *283*, 14453–14460.